Atmos. Chem. Phys. Discuss., 13, 11827–11862, 2013
www.atmos-chem-phys-discuss.net/13/11827/2013/
doi:10.5194/acpd-13-11827-2013

Atmospheric Chemistry and Physics Discussions

Transport of atmospheric NO_x and HNO_3 over Cape Town

B. J. Abiodun[1], A. M. Ojumu[2], S. Jenner[1], and T. V. Ojumu[3]

[1]Climate Systems Analysis Group, Department of Environmental and Geographical Science, University of Cape Town, South Africa
[2]Department of Environmental and Agricultural Sciences, University of South Africa, South Africa
[3]Department of Chemical Engineering, Peninsula University of Technology, South Africa

Received: 5 March 2013 – Accepted: 26 March 2013 – Published: 3 May 2013

Correspondence to: B. J. Abiodun (babiodun@csag.uct.ac.za)

Published by Copernicus Publications on behalf of the European Geosciences Union.

Abstract

Cape Town, the most popular tourist city in Africa, usually experiences air pollution with unpleasant odour in winter. Previous studies have associated the pollution with local emission of pollutants within the city. The present study examines the transport of atmospheric pollutants (NO_x and HNO_3) over South Africa and shows how the transport of pollutants from the Mpumalanga Highveld may contribute to the pollution in Cape Town. The study analysed observation data (2001–2008) from Cape Town air quality network and simulation data (2001–2004) from regional climate model (RegCM4) over southern Africa. The simulation accounts for the influence of complex topography, atmospheric condition, and atmospheric chemistry on emission and transport of pollutants over southern Africa. Flux budget analysis was used to examine whether Cape Town is a source or sink for NO_x and HNO_3 during the extreme pollution events.

The results show that extreme pollution events over Cape Town are associated with the low-level (surface–850 hPa) transport of NO_x from the Mpumalanga Highveld to Cape Town, and with a tongue of high concentration of HNO_3 that extends from the Mpumalanga Highveld to Cape Town along the south coast of South Africa. The prevailing atmospheric conditions during the extreme pollution events feature an upper-level (700 hPa) anticyclonic flow over South Africa and a low-level col over Cape Town. The anticyclonic flow induces a strong subsidence motion, which prevents vertical mixing of the pollutants and caps high concentration of pollutants close to the surface as they are transported from the Mpumalanga Highveld toward Cape Town, while the col accumulates the pollutants over the city. This study shows that Cape Town can be a sink for the NO_x and HNO_3 during extreme pollution events and suggests that the accumulation of pollutants transported from other areas (e.g. Mpumalanga Highveld) may contribute substantially to the air pollution in Cape Town.

ACPD
13, 11827–11862, 2013

1 Introduction

Accumulation of atmospheric mono-nitrogen oxides (NO_x) and its acid derivative (HNO_3) can have severe impacts on climate, environment, and human health. NO_x concentration in the atmosphere is essentially the total concentration of nitric oxide (NO) and nitrogen dioxide (NO_2), while the acid derivate, nitric acid (HNO_3), is an oxidative product of NO_x as shown in Eqs. (1)–(4).

$$NO + O_3 \rightarrow NO_2 + O_2 \quad (1)$$

$$NO_2 + O \rightarrow NO + O_2 \quad (2)$$

$$4NO + 3O_2 + 2H_2O \rightarrow 4HNO_3 \quad (3)$$

$$2NO_2 + H_2O \rightarrow HNO_2 + HNO_3 \quad (4)$$

The ratio of NO/NO_2 is determined by ozone availability, sunshine (or temperature); and nitric acid is produced from dissolution of NO_2 in moisture (Seinfeld and Pandis, 2006). Reaction of NO_x and sulphur dioxide in the presence of moisture produces acid rain which corrodes cars, buildings and historical monuments and makes streams and lakes acidic, uninhabitable for fish. Reaction of NO_x and ammonia with other substances generate particles and nitric acid. These particles have negative impacts on human respiratory system, damage lung tissue, and cause premature death. Small particles, in particular, can penetrate deeply into sensitive parts of the human lungs and cause respiratory disease such as emphysema and bronchitis; they can aggravate existing heart disease. Nitric acid corrodes and degrades metals (Dean, 1990). Excess nitrate is harmful to ecosystems because it can lead to "eutrophication", which deteriorates waters quality and kills fish. However, the complexity of nutrient cycling in ecosystems may make the long-term impact of nitric acid take decades to become apparent (Fields, 2004). Reaction of NO_x with volatile organic compounds (VOCs) in the presence of heat and sunlight produces ozone, a major component of smog. Smog and ozone are well known to cause nose and throat irritation and eventually death. Ozone can also damage vegetation and reduce crop yields. Cape Town, Africa's most

ACPD
13, 11827–11862, 2013

popular tourist city with about 3.5 million people (StatsSA 2009), is usually covered with smog (called brown haze) in winter. And several studies (e.g. Wicking-Baird et al., 1997) have linked the brown haze with unpleasant odours, health effects and visibility impairment in the city.

A combination of geographical and meteorological factors makes Cape Town favourable for accumulation of air pollutants. The location of Cape Town (33.9° S, 18.4° E) at the south-west tip of Africa (Fig. 1a) influences the wind patterns. The city is bordered by the Table Mountain complex to the south-west, False Bay to the south and Table Bay to the west. At this subtropical latitude, calm conditions are sometimes produced over the city under stagnant anticyclonic flows. The subsidence temperature inversion suppresses vertical exchange of air and pollutants during most periods of the year. In addition, radiative cooling at night produces stable layer at the surface to form surface inversion, which prevents the vertical dispersion of pollutants during the early mornings. The South Atlantic anticyclone and the cold Benguela current induce surface inversion, which strengths over the Cape Town (Preston-Whyte et al., 1977). Due to the temperature contrast between cold Bengula Current and the warm land weak, sea-breeze develops during the day and traps pollutant within the Cape Town basin. Berg winds, which occur when a high-pressure system over Kwazulu-Natal is associated with a high-pressure system over the Western Cape with an approaching cold front, favour brown haze episodes because the warm north-easterly reduces dew point temperature during the night (Jury et al., 1990). Consequently, extreme high pollution events occur from April to September; and whenever the brown haze occurs during this period, it extends over most of the Cape Town and shifts according to the prevailing wind direction (Wicking-Baird et al., 1997).

Many studies have investigated pollution over Cape Town, but their focuses have been on the influence of locally emitted pollutants. Wicking-Baird et al. (1997) showed that vehicles are the principal source of pollution in Cape Town, accounting for about 65 % of the brown haze. Low-level emitting industries also contribute considerably, accounting for about 22 % of the brown haze. The use of wood by a large sector of the

ACPD
13, 11827–11862, 2013

population accounts for about 11 % of brown haze Natural sources, such as wind-blown dust and sea salt, contribute about 2 % towards the brown haze. Walton (2005) identified Caltex Oil Refinery and Consol Glass as the main two point sources in the city, while the Cape Town Central Business District, Cape Town International Airport, and townships of Khayelitsha and Mitchell's Plain are the major area sources. However, the previous studies did not account for contribution of pollutants transported from remote sources to Cape Town. Since secondary pollutants like HNO_3 can be transported by wind to cause health impact far from their original sources, it is important to investigate how pollutants transported from remote sources in South Africa can contribute to the air quality problem in Cape Town. This paper addresses how NO_x and HNO_3 transported from the Mpumalanga Highveld (the most industrialized region in South Africa) can accumulate over Cape Town.

The Mpumalanga Highveld accounts for 90 % of South Africa's emission of nitrogen oxides and other gases (Collett et al., 2010). Previous studies (Freiman and Piketh 2003; Piketh et al., 2002) have considered regional scale transport and recirculation of pollutants emitted from the Highveld (using trajectory models with reanalysis data with low resolution) and showed that most of pollutants from the Highvield pollutants are transported to Indian Ocean by the westerlies at 700 hPa. However, since the Mpumalanga Highveld is located north-east of Cape Town, a persistent low-level north-easterly flow over South Africa can transport the pollutants from Highveld to Cape Town. Such a transport may not be captured by the previous studies, which used low resolution atmospheric data in trajectory models. In addition, the trajectory models cannot account for chemical reactions that occur among the pollutants during the transports, making it is difficult to account for the concentration of primary and secondary pollutants separately. Meanwhile, in some cases, the concentration of the secondary pollutants may be higher than that of their precursors. In the present study, a high resolution atmospheric-chemistry model that accounts for influence of topography, atmospheric condition, and chemical reactions among the atmospheric gasses is used to investigate the transport of pollutants from the Mpumalanga Highveld to Cape Town.

ACPD
13, 11827–11862, 2013

The aim of this paper is to study the transport of NO_x and NHO_3 over South Africa and investigate how pollutants from the Mpumalanga Highveld may contribute to air pollution in Cape Town. The study combines analysis of station observations and regional climate model simulation to achieve the aim. It calculates the flux budget of the pollutants over Cape Town and investigates the atmospheric conditions that favour accumulation of pollutants over the city. The methodology used in the study is present Sect. 2, results and discussions are in Sect. 3, while the conclusion is in Sect. 4.

2 Methodology

2.1 Observed data

This study used meteorological and pollution data from four stations within the Cape Town Air Quality monitoring network (Fig. 1b). The network comprises of 12 stations within 500 km^2 area and measures ambient concentrations of selected pollutants considered hazardous to human health and ecology (City of Cape Town, 2005), as well as relevant meteorological parameters that might explain high concentrations. The stations with relevant observations for the period of the study are City Hall, Goodwood, Bothasig and Tableview (Fig. 1b). Vehicular emissions are the prime source of pollution for the City Hall station, which is located opposite the city's busy taxi rank, bus station and rail terminus. Goodwood is a mixed residential and commercial area with nearby industry to the south east and south west. The nearby national road, the N2, carries commuter traffic from Cape Town's northern suburbs to the City, and another busy national road, the N7, passes along the south side of this area. Road traffic near these two stations is congested during the morning and evening commute. Although near arterial roads, traffic is a less source for the Bothasig and Tableview monitors located near the coast and in close proximity to each other.

The data used for this study comprises the hourly average of NO, NO_2 and NO_x concentrations, wind speed, wind direction and temperature for 10 yr (2000–2009). The

ACPD
13, 11827–11862, 2013

data were analysed to identify temporal variation of concentrations and associated atmospheric condition to the peaks. Diurnal variation was analyzed to investigate the concentration peaks and the contribution of the atmospheric conditions. Monthly mean concentration of pollutants and climatological variables were used to identify the influence of seasonal variation. Monthly temperature and rainfall data from the Climate Research Unit (CRU; Mitchell and Jones, 2005) were analyzed to supplement the station data in validating model simulation.

2.2 Models description and set-ups

The study applied the International Centre for Theoretical Physics (ICTP) Regional Climate model (version 4) with chemistry (hereafter, RegCM) to simulate the climate and pollution transport over Southern Africa (Fig. 2). The model allows online coupling of atmospheric and chemistry parameters. The climate component has been successfully tested over Southern Africa (Sylla et al., 2009). RegCM is a hydrostatic, sigma-coordinate model (Pal et al., 2007; Giorgi et al., 2012). The model has various options for physics and chemistry parameterisations. In the present study, the model used the CCM3 (Kiehl et al., 1996) radiation scheme for radiation calculations, the (Grell et al., 2005) mass-flux cumulus scheme with Fritsch and Chappell (1980) closure for convection, and the Holtslag and Boville (1993) scheme for planetary boundary layer parameterisation. Surface layer land-atmosphere interactions were represented with BATS1E (Biosphere-Atmosphere Transfer Scheme) (Dickinson et al., 1993), which is based on Monin Obukhov similarity relations (Monin and Obukhov, 1954). For the chemistry routines, the photochemical Carbon Bond Mechanism-Z (CBM-Z) (Zaveri and Peters, 1999) was used. Photolysis is based on the Tropospheric Ultraviolet-Visible Model (TUV) scheme developed by Madronich and Flocke (1999). For dry deposition the model used the CLM4 (Community Land Model 4) developed after Wesley (1989) and wet deposition follows the MOZART global model (Emmons et al., 2010). Shalaby et al. (2012) present a detailed description of the gas-phase chemistry in RegCM.

ACPD
13, 11827–11862, 2013

The RegCM simulation was set up with a 35 km horizontal resolution. The simulation domain centres on 33° S and 24° E and extends, with the Lambert conformal projection, from 16.62° W to 54.41° E and from 10.5° S to 40.45° S (Fig. 2). In the vertical, the domain spans 18 sigma levels, with highest resolution near the surface and lowest resolution near the model top. Initial and lateral boundary meteorological conditions were provided by ERA-Interim 1.5° × 1.5° gridded reanalysis data from ECMWF (European Centre for Medium-Range Weather Forecasts). Emissions data with a 1° × 1° resolution was provided by the RCP (Representative Concentration Pathways) global dataset that accompanies the standard RegCM package. The simulation covers a period of 4 yr 3 months (i.e. October 2000–December 2004). The first 3 months simulations were discarded as model spin-up, while the remaining four years simulations were analysed for the study.

2.3 Pollutants flux budget

Flux budget analysis was use to calculate net flux of the pollutants (NO_x and HNO_3) over the Cape Town and to examine whether city is a source or sink for the pollutants. The net flux (F_{Net}) is defined as:

$$F_{Net} = (F_E - F_W) + (F_N - F_S); \quad (5)$$

where F_E, F_W, F_N, and F_S are the pollutant fluxes at the east, west, north and south boundaries of Cape Town (Fig. 1a), respectively. A positive zonal flux (F_E or F_W) implies a westerly pollutant flux (i.e. pollutant flux from the west direction) while a negative zonal flux means the opposite. A positive meridional flux (F_N or F_S) denotes a southerly pollutant flux (i.e. pollutant flux from the south direction) while a negative zonal flux means the opposite. A positive net flux indicates divergence of a pollutant over the city, meaning that the city is a net source for the pollutant. A negative net flux indicates convergence (or accumulation) of pollutants over the city, meaning that the city is net sink for the pollutant.

ACPD
13, 11827–11862, 2013

3 Results and discussion

This section presents and discusses the results of the study in three parts. The first part describes the temporal (diurnal and seasonal) variation of the observed pollutant concentrations and meteorological variables at the four stations (City Hall, Goodwood, Bathasig and Tableview) within the city (see Fig. 1b). The second part compares RegCM simulation (pollutant concentrations and meteorological variables) with the observed data. The third part discusses the characteristics of the simulated NO_x (NO and NO_2) and HNO_3 over Cape Town.

3.1 Observed nitrogen oxides and atmospheric condition over Cape Town

3.1.1 Diurnal variation

The diurnal cycle of the NO, NO_2, NO_x (Fig. 3) shows that the pollutants have the highest concentration at City Hall and the lowest concentration at Tableview. This is because City Hall is located in the heart of the city where emission of NO from daily anthropogenic activity (traffic, industrial, business) is greatest. The diurnal variation of NO concentration (Fig. 3a) shows two peaks (morning and evening peaks) at City Hall but one peak (in morning) at other stations (Bothasig, Goodwood, and Tableview). The morning peaks (City Hall: 280 $\mu g\,m^{-3}$; Goodwood: 120 $\mu g\,m^{-3}$; Bothasig: 60 $\mu g\,m^{-3}$; and Tableview: 20 $\mu g\,m^{-3}$) occur at 08:00 SLT while the evening peak (City Hall: 60 $\mu g\,m^{-3}$) occurs at 16:00 SLT. Although Bothasig, Goodwood, and Tableview show no evening peak, the NO concentration is higher in the evening (18:00–20:00) than in the afternoon. The morning peaks, and the evening peak at City Hall, can be attributed to the high commuter traffics in the city, because people rush to work and school in the morning (around 08:00 SLT) and return home in the evening (16:00 SLT). However, the concentration peak is higher in morning than in the evening because the traffic rush is greater in the morning than in the evening, as schools and offices open at same time in the morning (08:00 SLT) but close as different time in the afternoon.

ACPD
13, 11827–11862, 2013

The diurnal variation of NO_2 differs from that of NO. At City Hall, the diurnal variation of NO_2 shows no distinct peak; instead, it shows a uniform concentration (about 50 $\mu g\,m^{-3}$) during the day (08.00–18.00 SLT) and a lower concentration (about 20 $\mu g\,m^{-3}$) at night. In contrast, the diurnal variation of NO shows two distinct peaks at other stations (Goodwood: 25 $\mu g\,m^{-3}$; Tableview and Bathasig: 18 $\mu g\,m^{-3}$), in morning (08:00 SLT) and evening (19:00 SLT). However, at all stations, the NO_2 concentration is smaller than that of NO, possibly because NO_2 is a secondary reaction product of NO and oxygen (Eq. 1); the reaction rate is slow and depends on favourable atmospheric condition. Nevertheless, since the magnitude NO concentration is about 5 times higher than that of NO_2, the diurnal variation of NO_x ($NO + NO_2$) follows that of NO.

However, the diurnal variation of meteorological variables may also play an important role on that the diurnal variation of the pollutants concentration. The diurnal variation in wind speed (Fig. 3e) and surface temperature (Fig. 3d) may enhance the concentrations of the pollutants in the morning and lower it in the afternoon. For instance, the weak surface wind speed in the morning (Fig. 3b) may lead to accumulation and higher concentration of NO concentration, while the higher wind speed in the afternoon may reduce NO concentration. Besides, in the morning, the surface inversion layer (induced by low surface temperature from the nocturnal radiative cooling) can inhibit vertical mixing of the NO. In the afternoon, the surface heating increases the surface temperature and the development of mixing layer will erode the inversion layer. Hence, pollutants trapped below the surface layer will rise and disperse, reducing the NO concentration in the afternoon. In contrast, the increase in NO_2 concentration in afternoon may be attributed to increase in temperature which can enhance generation of more NO_2 due to chemical reaction (see Eq. 1). This could further explain why NO_2 concentration is much higher at City Hall (where maximum temperature is about 27 °C) than at Bothasig (where the maximum temperature is about 22 °C).

ACPD
13, 11827–11862, 2013

3.1.2 Seasonal variation

The concentration of the pollutants also varies with seasons (Fig. 3). Since the anthropogenic emission of NO in Cape Town hardly changes with seasons, the seasonal variations of the atmospheric condition must play a major role in the seasonal variation of the pollutants concentration. At all stations, NO shows a maximum concentration (City Hall, 200 $\mu g\,m^{-3}$; Goodwood, 100 $\mu g\,m^{-3}$; Bothasig, 100 $\mu g\,m^{-3}$; Tableview, 30 $\mu g\,m^{-3}$) in early winter (June) and a minimum concentration (City Hall: 80 $\mu g\,m^{-3}$; Goodwood, Bothasig and Tableview: 20 $\mu g\,m^{-3}$) in summer (December–February). Nevertheless, the seasonal variation is most pronounced at City Hall and least defined at Tableview (Fig. 3a). The occurrence of maximum concentration of NO in winter can be attributed to the weak wind speed and low surface temperature during this period, as both conditions do not favour the pollutant dispersion and its conversion to NO_2 through the reaction in Eq. (1).

The seasonal variation of NO_2 (and NO_x) is similar to that of NO, except that: (1) the concentration of NO_2 is smaller than that of NO; (2) at City Hall, the maximum concentration of NO_2 extend over more months (March–July) than that of NO; and (3) at Tableview, the maximum concentration of NO_2 is in March–May instead of in June (as for NO). The occurrence of maximum concentration of NO_2 in March–July can be attributed to a balance between NO concentration and atmospheric condition that favours NO_2 production. For instance, less NO concentration limits the production of NO_2 in January (when the temperature is most favourable for the production), and less favorable atmospheric condition prevents a peak concentration of NO_2 in June, when the NO concentration reaches the peak.

3.2 Model validation

The daily mean concentration of the simulated NO shows a weak correlation with the observed values and the standard deviation is lower than the observed (Fig. 5). The correlation coefficient is about 0.4 and the normalized standard deviation is 0.4. The

ACPD
13, 11827–11862, 2013

simulated correlation between the observed and simulated NO_2 is also 0.4, but the normalized standard deviation (about 1.0) is much better than that of NO. The normalized standard deviation of NO_x (0.50) falls between those of NO and NO_2, but the correlation coefficient is also 0.4. There is a better correlation between the simulated and observed atmospheric variables than with the pollutants, suggesting that the weak correlation between the observed and simulated pollutant concentration may be due to the RegCM chemistry. However, the RegCM shows its best performance in simulating temperature, the correlation coefficient is 0.85 and the normalized standard deviation is 0.8.

The seasonal variation of the simulated pollutants concentrations resembles that of the observation, but with some biases in the values (Fig. 6). The model underestimates the concentrations of NO and NO_x in winter (May–August) and overestimates them in other months. It underestimates NO_2 concentration in March–September and overestimates it in other month. For all the pollutants, the highest bias in the simulation occurs in June and the lowest bias is in April or September. The peaks of the simulated concentrations (in April) are two months earlier than the observed (June). The decrease in the simulated pollutant concentration in winter may be attributed to the winter rainfall, which cleanses the atmosphere of any accumulated pollutant. The simulated rainfall and temperature show a good agreement with CRU observation, except that the model underestimates temperature in summer months, overestimates rainfall in winter and underestimates rainfall in winter. Another discrepancy between the simulation and observation is in that the relationship between NO and NO_2 is stronger in the simulation than in observation.

ACPD
13, 11827–11862, 2013

3.3 Characteristics of the simulated pollutant and atmospheric condition over South Africa

3.3.1 Annual mean

RegCM simulates the hot spots of NO, NO_2 and HNO_3 concentrations over the north-east South Africa (Fig. 7). The maximum concentration of NO (about $30 \times 10^{-6}\,g\,kg^{-1}$) is over the Mpumalanga Highveld, the area of intense industrial activities in South Africa (Collett et al., 2010). The maximum concentration of NO_2 (about $5. \times 10^{-6}\,g\,kg^{-1}$) is also over the Mpumalanga Highveld, but the magnitude is lower than that of NO, because NO_2 forms from the reaction of NO with other substances (see Eq. 1); the reaction depends on the availability of those substances and on the atmospheric condition. The maximum concentration of HNO_3 (about $5. \times 10^{-6}\,g\,kg^{-1}$) is also lower than that of NO, but HNO_3 concentrations cover a wider area than those of NO and NO_2 concentrations. For instance, the contour of $0.5 \times 10^{-6}\,g\,kg^{-1}$ in HNO_3 covers almost the entire country, but that of NO and NO_2 are limited to the eastern part of the country (Fig. 7). This is because most of the NO and NO_2 are converted to HNO_3 as they are transported away from the hot spots.

The model simulation shows a difference in the transport of the pollutants (NO, NO_2 and HNO_3) at low level (surface – 850 mb) and at upper level (700–500 mb) (Fig. 7). At the upper level (i.e. 700 hPA), the wind pattern is dominated by a westerly flow with a weak trough over the western coast and an anti-cyclonic flow over the north-east South Africa. At this level, the westerly flow transports most pollutants from the hot spots towards the Indian Ocean while the anticyclonic flow recycles the pollutant over southern Africa But, at low level, the wind pattern is dominated by northerly and north-easterly flows over the continent, south-westerly and south-easterly flows over the Atlantic Ocean, and easterly flows over the Indian Ocean. The northerly and north-easterly flows transport pollutants from the hot-spots toward the southern coast and to Cape Town. The northerly flows converge with the southerly winds along the southern

ACPD
13, 11827–11862, 2013

coasts. The convergence produces weak winds and induces accumulation of the pollutants over the south-western half of the South Africa, along the southern coasts, and over Cape Town. The easterly flow transports fresh air from the Indian Ocean to the eastern coast, but also picks pollutants from the hot spots and transports them along the coastline towards Cape Town area. Hence, while the upper level winds (westerlies) transport fresh-air eastward from Atlantic Ocean over Cape Town area, the surface winds (easterlies and north-easterlies) transport pollutants from the Mpumalanga Highveld toward the city.

The emphases of previous studies have been on the eastward transport of Highveld pollutants by the upper-level westerly flow and on the recirculation of the pollutants over southern Africa by the anti-cyclones. For instance, Freiman and Piketh (2003) show that 39 % of pollutants from the Highveld are transported to the Indian Ocean, 33 % are recycle over the sub-continent, and only 6 % are transported by the northerly flow to the south of Indian ocean. But the present results suggest that the amount of HNO_3 transported from the Highveld pollutants southward (and towards Cape Town) may be substantial. And given that the winds are weaker at low level than at upper level, and the pollutant concentrations are higher at low-level than at upper-level, it important to have a better understanding of pollutants transport at low-level, especially over South Africa. Using a high resolution (about 1.5 × 1.5 km) simulation over Western Cape, Jury et al. (199) attributes the weak wind over western cape to convergence of land and sea breeze; but the present study suggests that the weak wind may be due to convergence of synoptic scale flows because the lower resolution (30 × 30 km) simulation used in the present study cannot resolve land and sea breeze, yet the simulation features the weak wind and further shows that weak wind covers a wider domain than shown in Jury et al. (1990).

3.3.2 Seasonal variation

The simulated HNO_3 over South Africa exhibits a seasonal variability, in which atmospheric condition plays a major role (Fig. 8). The highest variability in HNO_3 occurs

ACPD
13, 11827–11862, 2013

over the Mpumalanga Highveld, with positive anomalies in April–September and negative anomalies in October–March. The anomalies can be attributed the prevailing atmospheric condition during the periods. In summer (October–January), the inversion layer over the eastern coast is elevated above the mountain range (i.e. the escarpment). This allows the easterly flow from the Indian Ocean to penetrate inland and dilute the concentration of HNO_3 over the Mpumalanga Highveld (Fig. 9). The reverse is the case in winter (April–August), when the inversion layer is lower than the peak of the escarpment. The easterly flow cannot penetrate inland with the fresh air; instead, it deflects around the mountain ranges, southward along the coastline or northward toward Mozambique. Rainfall may also lower HNO_3 concentration in summer, because the eastern part of South Africa experiences intense rainfalls in summer and the rainfall will cleanse the atmosphere of HNO_3.

The seasonal variation of HNO_3 is weaker over Cape Town than over the Mpumalanga Highveld, but the anomalies over Cape Town are substantial and are influenced by transport of HNO_3 from the Mpumalanga Highveld region. The seasonal variability shows strong positive anomalies of HNO_3 in February–April and weaker negative anomalies in other months. The months with the positive anomalies feature easterly and north-easterly flows transporting HNO_3 from the Mpumalanga Highveld toward Cape Town, while the months with negative anomalies are characterized by south-westerly transporting fresh maritime air towards Cape Town. The removal of HNO_3 from the atmosphere by winter rainfall may contribute to the negative anomalies in winter months.

Table 1 presents the monthly budget of pollutants (NO, NO_2, NO_x and HNO_3) fluxes over Cape Town at low level. The monthly mean of the net flux is positive for all the pollutants in each month. That means that, over the city, the magnitude of outgoing pollutants is greater than magnitude of incoming pollutants; so, Cape Town is a source for the pollutants. For all the pollutants, the maximum net flux occurs in April and the minimum in November, January, or August. The west boundary of the city always experiences outward fluxes of the pollutants, except in June when it experiences inward fluxes

ACPD
13, 11827–11862, 2013

of HNO_3 (Table 1); its maximum outward flux occurs in January. The north boundary features inward fluxes for the pollutants in April–August but outward fluxes in the remaining months. The reverse is the case at south boundary, where there are outward fluxes in April–August but inward fluxes in other months. However, in most cases, the magnitudes of the outward fluxes at the west boundary are greater than the magnitude of outward or inward fluxes at other boundaries. Hence, climatologically, Cape Town is a net exporter of the pollutants, and most of the pollutants from the city are exported through the west boundary. However, as it will be shown later, the situation is different during extreme pollution events.

3.3.3 Transport of pollutant during extreme events in Cape Town

The time series of the simulated pollutants concentration over Cape Town (Fig. 10) shows that the extreme concentration events (defined as 99 percentiles; $\geq 3.3 \times 10^{-6}\,g\,kg^{-1}$ for NO_x; $\geq 2.8 \times 10^{-6}\,g\,kg^{-1}$ for HNO_3) mostly occur in April. For NO_x (Fig. 9c), the extreme events occur once in 2001 but twice in 2003 and 2004. For HNO_3, the extreme events occur once 2001, thrice in 2002 and twice in 2003 and 2004. However, the extreme event for NO_x and HNO_3 rarely occur on the same day, suggesting that, in Cape Town, the atmospheric conditions that induce NO_x extreme events may be different from those that induces of HNO_3 extreme events.

The composite of wind flow during extreme pollution events in Cape Town shows a transport of pollutant from the Mpumalanga Highveld to Cape Town at surface (Fig. 11). For NO_x extreme events, the low-level wind pattern is characterized with northerly and north-easterly flows, transporting the pollutant from the Mpumalanga Highveld towards Cape Town and south coast. Along the south coastline, there is a confluence of the northerly flow and easterly flow; and the easterly flow also transports pollutants from eastern part of South Africa towards Cape Town. The wind pattern also features a col over Cape Town. A col is a relatively neutral area of low pressure between two anticyclones, or a point of intersection of a trough (in cyclonic flow) and a ridge (in anti-cyclonic flow). It usually associated with a calm or light variable wind which causes

ACPD
13, 11827–11862, 2013

stagnation of air flow. Since a col cause can accumulation of atmospheric pollution (Stein et al., 2003), the formation of a col with the convergence of north-easterly and southerly over Cape Town will provide a favourable atmospheric condition for accumulation of the pollutants over the city during the extreme events. At 700 hPa (Fig. 12), there is a strong anticyclonic flow over southern Africa. This anticyclone will produce a strong subsidence over South Africa, and the subsidence will prevent a vertical mixing of the pollutants, capping the high concentrations of pollutants close to the surface as they are transported toward from the Mpumalanga Highveld toward Cape Town.

The synoptic wind patterns that induce the extreme HNO_3 events differ from those that induce the extreme NO_x events (Fig. 11d). With HNO_3 extreme event, the low-level wind pattern features a strong north-westerly flow transporting HNO_3 from the Mpumalanga Highveld towards the south coast. In addition, it shows a strong easterly flow transporting fresh air from Indian Ocean, but turns poleward as it approaches the escarpment, thereby deflecting the fresh air from the continent, at same time, forming a confluence flow with the north-westerly flow along the coast. The wind patterns also feature a weak wind along the south coast and a col over Cape Town. Hence, there is a band of high HNO_3 concentration along the coast, linking the peak HNO_3 concentration at Cape Town with that over the Mpumalanga Highveld. As with NO_x extreme event, the 700 hPa wind pattern features a strong anticyclone (centering over the border between South Africa and Botswana) but with a stronger north-westerly flow over the western flank of South Africa.

Table 2 shows that Cape Town is a sink for all the pollutants during the extreme events, except for HNO_3 in March and April. For NO_x (NO and NO_2), while the west boundary experiences outward fluxes, the east and north boundaries experience inward fluxes with higher magnitudes than the outward fluxes at the west boundary. The direction of the fluxes at the south boundary varies: inward fluxes for NO in March, NO_2 in March and April, but outward fluxes NO and NO_x in April. Nevertheless, net fluxes for NO_x (NO and NO_2) are negative, meaning accumulation of NO_x (NO and NO_2) over the city, during the extreme event. The characteristics of HNO_3 fluxes during the extreme

ACPD
13, 11827–11862, 2013

events differ from (and more complex than) that of NO_x. For HNO_3, the west and north boundaries experience inward fluxes during the extreme events in March and May but outward fluxes in April. The east boundary experiences outward fluxes of HNO_3, while the south boundary experiences and inward fluxes in April but outward fluxes in March and May. Nevertheless, the table indicates an accumulation of HNO_3 over Cape Town in May, though not March and April.

4 Conclusions

As part of ongoing efforts to understand the sources of pollution in Cape Town, this study has applied a regional climate model (RegCM) to study the transport of NO_x and HNO_3 over South Africa, with emphasis on pollutants transport from Mpumalanga Highveld to Cape Town. It also examines whether Cape Town is a net sink or source for the pollutants. The model accounts for the influence of southern African complex topography, atmospheric condition and pollutant chemical reactions in simulating the emission, dispersion and transport of the pollutants. The study described the characteristic of observed NO and NO_2 over Cape Town, examined how well the regional model captures the characteristics, and analyzed the model simulations to describe the influence of atmospheric condition on the seasonal variations of the pollutants over South Africa. It calculated the flux budget of the pollutant over the city for each month and for composite of days with extreme pollution event.

The diurnal variation of NO_x over Cape Town exhibits two peaks (morning and evening peak) mainly due to traffic rush, but the atmospheric condition also play a critical role on the morning peak. The seasonal variation is more influenced by changes in the atmospheric condition than changes in the local emissions from traffics or industries. The model captures the seasonal variation of NO_x (NO and NO_2) concentration as observed, except that it underestimates the anomalies in May–June. The correlation coefficient between the observed and simulated daily concentration of the pollutants is

ACPD
13, 11827–11862, 2013

about 0.4 while the normalized standard deviation varies between 0.4 and 1.0; the model performs better in simulating the atmospheric variables.

While the results of this study agree with those from previous studies that the Mpumalanga Highveld's pollutants are transported eastward by the westerly flow at 700 hPa, it shows that the reverse is the case at low-level (surface–850 hPa) where the concentration of the pollutant is higher. At the low-level the easterly and north-easterly flows transport the Mpumalanga Highveld's pollutants westward toward to Cape Town. And during the extreme events, the north-easterly flow transports NO_x directly from The Mpumalanga Highveld to Cape Town, a band high concentration of HNO_3 links the peak HNO_3 concentration at Cape Town with that of The Mpumalanga Highveld, and the 700 hPa synoptic winds features a strong anticyclone that induces strong subsidence over South Africa. The formation of col over Cape Town during the extreme event makes the city conducive for accumulation of pollutants. However, the pollutants budget flux over Cape Town shows that could be a net source or net sink for NO_x and HNO_3 during the extreme events.

Since these results are based on four years simulation from one model, there is need for longer simulations with multi-models to establish the robustness of the findings. A longer simulation will account for the influence inter-annual variability on the results while using multi-model simulations will provide opportunity for models comparisons and for assessing the degree of inter-model variability. However, the present study suggests that the transport of NO_x and HNO_3 from Mpumalanga Highveld may contribute to the pollutants concentration in Cape Town.

Acknowledgement. The project was supported with grants from National Research Foundation (NRF, South Africa) and the Applied Centre for Climate and Earth Sciences (ACCESS). The third author was supported with grants from African Centre for Cities (ACC). Computations facility was provided by Centre for High Performance Computing (CHPC, South Africa).

ACPD
13, 11827–11862, 2013

References

Collett, K. S., Piketh, S. J., and Ross, K. E.: An assessment of the atmospheric nitrogen budget on the South African Highveld, S. Afr. J. Sci., 106, 1–9, 2010.

City of Cape Town: Air Quality Management Plan for the City of Cape Town, Cape Town, 2005.

Dean, S. W.: Corrosion testing of metals under natural atmospheric conditions, in: Corrosion Testing and Evaluation, Silver Anniversary Volume, 163–176, ASTM, Philadelphia, PA, 1990.

Dickinson, R. E., Henderson-Sellers, A., and Kennedy, P. J.: Biosphere-atmosphere transfer scheme (BATS) version 1e as coupled to the NCAR community climate model, technical report, Boulder, Colorado, 1993.

Emmons, L. K., Walters, S., Hess, P. G., Lamarque, J.-F., Pfister, G. G., Fillmore, D., Granier, C., Guenther, A., Kinnison, D., Laepple, T., Orlando, J., Tie, X., Tyndall, G., Wiedinmyer, C., Baughcum, S. L., and Kloster, S.: Description and evaluation of the Model for Ozone and Related chemical Tracers, version 4 (MOZART-4), Geosci. Model Dev., 3, 43–67, doi:10.5194/gmd-3-43-2010, 2010.

Fields, S.: Cycling out of control, Environ. Health Persp., 112, 556–563, 2004.

Freiman, M. T. and Piketh, S. J.: Air transport into and out of the industrial Highveld region of South Africa, J. Appl. Meteorol., 42, 994–1002, 2003.

Fritsch, J. M. and Chappell, C. F.: Numerical prediction of convectively driven mesoscale pressure systems, part I: convective parameterization, J. Atmos. Sci., 37, 1722–1733, 1980.

Giorgi, F. and Anyah, R. O.: The road Towards RegCM4, Clim. Res., 52 3–6, 2012.

Grell, G. A., Peckham, S. E., Schmitz, R. McKeen, S. A. Frost, G., Skamarock, W. C., and Edere, B.: Fully coupled online chemistry within the WRF model, Atmos. Environ., 39, 6957–6975, 2005.

Holtslag, A. A. M. and Boville, B. A.: Local versus nonlocal boundary-layer diffusion in a global climate model, J. Climate, 6, 1825–1842, 1993.

Jury, M., Tegen, A., Ngeleza, E., and Dutoit, M.: Winter air pollution episodes over Cape Town, Bound.-Lay. Meteorol., 53, 1–20, 1990.

Kiehl, J. T., Hack, J. J., Bonan, G. B., Boville, B. A., Breigleb, B. P., Williamson, D., and Rasch, P.: Description of the NCAR community climate model (CCM3), Technical report NCAR/TN-420+STR, Boulder, Colorado, 1996.

Madronich, S. and Flocke, S.: The role of solar radiation in atmospheric chemistry, in: Handbook of Environmental Chemistry, edited by: Boule, P., Springer-Verlag, New York, 1–26, 1999.

ACPD
13, 11827–11862, 2013

Monin, A. S. and Obukhov, A. M.: Osnovnye zakonomernosti turbulentnogo peremesivanija v prizemnom sloe atmosfery y (Basic laws of turbulent mixing in the atmosphere near the ground), Trudy Institute Geologicheskikh Geofizi, 24, 163–187, 1954.

Mitchell, T. D. and Jones, P. D.: An improved method of constructing a database of monthly climate observations and associated high-resolution grids, Int. J. Climatol., 25, 693–712, 2005.

Pal, J. S., Giorgi, F., Bi, X., Elguindi, N., Solmon, F., Gao, X., Rauscher, S. A., Francisco, R., Zakey, A., Winter, J., Ashfaq, M., Syed, F. S., Bell, J. L., Diffenbaugh, N. S., Karmacharya, J., Konare, A. Martinez, D., de Rocha, R. P., Sloan, L. C., and Steiner, A. L.: Regional climate modeling for the developing world: the ICTP RegCM3 and RegCNET, B. Am. Meteorol. Soc., 88, 1395–1409, 2007.

Piketh, S. J., Swap, R. J., Maenhaut, W., Annegarn, H. J., and Formenti, P.: Chemical evidence of long-range atmospheric transport over southern Africa, J. Geophys. Res., 107, 1–13, 2002.

Preston-Whyte, R. A., Diab, R. D., and Tyson, P. D.: Towards an inversion climatology of southern Africa, II, non-surface inversions in the lower atmosphere, S. Afr. Geogr. J., 59, 47–59, 1977.

Seinfeld, J. H. and Pandis, S. N.: Atmospheric Chemistry and Physics: From Air Pollution to Climate Change, 2nd edn., J. Wiley, New York, 2006.

Shalaby, A., Zakey, A. S., Tawfik, A. B., Solmon, F., Giorgi, F., Stordal, F., Sillman, S., Zaveri, R. A., and Steiner, A. L.: Implementation and evaluation of online gas-phase chemistry within a regional climate model (RegCM-CHEM4), Geosci. Model Dev., 5, 741–760, doi:10.5194/gmd-5-741-2012, 2012.

Stats, S. A.: Census 2001: Cape Town Profile, Cape Town, Statistics South Africa, available at: http://www.capetown.gov.za/en/stats/2001census/Documents/Cape%20Town.htm, last access: 23 May 2012, 2003.

Stein, D. C., Swap, R. J., Greco, S., Piketh, S. J., Macko, S. A., Doddridge, B. G., Elias, T., and Bruintjes, R. T.: Haze layer characterization and associated meteorological controls along the eastern coastal region of southern Africa, J. Geophys. Res., 108 , 1–11, 2003.

Sylla, M. B., Coppola, E., Mariotti, L., Giorgi, F., Ruti, P. M., Dell'Aquila, A., and Bi, X.: Multiyear simulation of the African climate using a regional climate model (RegCM3) with the high resolution ERA-interim reanalysis, Clim. Dynam., 35, 231–247, 2009.

ACPD
13, 11827–11862, 2013

Walton, N. M.: Characterisation of Cape Town Brown Haze, University of the Witwatersrand, Johannesburg, 2005.
Wesley, M. L.: Parameterization of surface resistance to gaseous dry deposition in regional-scale numerical models, Atmos. Envir., 23, 1293–1304, 1989.
Wicking-Baird, M. C., De Villiers, M. G., and Dutkiewicz, R.: Cape Town brown haze study, Report No. Gen. 192, Cape Town, 1997.
Zaveri, R. A. and Peters, L. K.: A new lumped structure photochemical mechanism for long-scale applications, J. Geophys. Res., 30, 387–415, 1999.

ACPD
13, 11827–11862, 2013

Table 1. The low-level flux budget of pollutants (NO, NO_2, NO_x and HNO_3) over Cape Town for each month, showing the inward and outward fluxes at the west (F_W), east (F_E), south (F_S) and north (F_N) boundaries of Cape Town and the net flux (F_{Net}) over the city. A positive zonal flux (F_E or F_W) implies a westerly flux (i.e. a flux from west direction) while a negative zonal flux means the opposite. A positive meridional flux (F_N or F_S) denotes a southerly flux (i.e. a flux from south direction) while a negative zonal flux means the opposite. Inward fluxes (from any boundary or direction) into the city are in red, while outward fluxes from the city are in black. A positive F_{Net} indicates divergence (i.e. depletion) of the pollutants over the city while a negative net flux means convergence (i.e. accumulation) of the pollutants over the city.

	Jan	Feb	Mar	Apr	May	Jun	Jul	Aug	Sep	Oct	Nov	Dec
NO												
F_W	−1.9	−2.4	−2.2	−1.3	−0.6	0.0	−0.4	−0.3	−1.1	−1.1	−1.6	−1.7
F_E	−0.4	−1.0	−0.8	0.3	0.5	0.9	0.6	0.9	0.2	0.2	−0.2	−0.4
F_S	1.6	1.5	1.5	−0.4	−0.7	−1.5	−1.2	−0.6	0.3	0.4	1.5	1.4
F_N	1.2	1.0	1.6	−0.2	−0.3	−0.7	−0.6	−0.3	0.1	0.4	1.0	1.2
F_{Net}	**1.1**	**0.9**	**1.5**	**1.7**	**1.5**	**1.7**	**1.6**	**1.5**	**1.2**	**1.3**	**0.9**	**1.0**
NO_2												
F_W	−1.5	−2.0	−1.8	−1.0	−0.5	0.0	−0.4	−0.3	−0.9	−0.9	−1.3	−1.4
F_E	−0.3	−0.6	−0.4	0.2	0.3	0.5	0.3	0.4	0.0	0.1	−0.2	−0.2
F_S	1.2	1.2	1.2	−0.3	−0.5	−1.0	−0.7	−0.4	0.2	0.3	1.1	1.0
F_N	0.8	0.8	1.0	−0.1	−0.2	−0.4	−0.4	−0.2	0.1	0.3	0.7	0.8
F_{Net}	**0.9**	**1.0**	**1.2**	**1.4**	**1.1**	**1.0**	**1.0**	**0.9**	**0.8**	**1.0**	**0.8**	**0.8**
NO_x												
F_W	−3.4	−4.4	−4.0	−2.2	−1.1	−0.1	−0.8	−0.6	−2.0	−2.0	−2.9	−3.0
F_E	−0.7	−1.5	−1.2	0.5	0.8	1.3	1.0	1.3	0.2	0.2	−0.4	−0.6
F_S	2.8	2.7	2.7	−0.7	−1.2	−2.5	−1.9	−1.0	0.5	0.6	2.5	2.5
F_N	1.9	1.8	2.6	−0.3	−0.6	−1.1	−1.0	−0.5	0.2	0.6	1.7	1.9
F_{Net}	**1.9**	**1.9**	**2.7**	**3.1**	**2.6**	**2.8**	**2.6**	**2.3**	**2.0**	**2.2**	**1.7**	**1.9**
HNO_3												
F_W	−3.1	−4.7	−3.7	−1.5	−0.8	0.2	−0.6	−0.5	−2.2	−1.6	−2.6	−2.8
F_E	−1.7	−3.0	−1.6	0.0	0.0	0.6	0.0	0.2	−1.2	−0.7	−1.1	−1.5
F_S	2.8	3.4	3.0	−0.4	−0.7	−1.7	−1.6	−0.7	0.7	0.7	2.5	2.6
F_N	1.8	2.1	2.2	−0.3	−0.6	−1.2	−1.7	−0.6	0.0	0.4	1.6	1.7
F_{Net}	**0.4**	**0.4**	**1.2**	**1.6**	**1.0**	**0.9**	**0.6**	**0.8**	**0.4**	**0.6**	**0.5**	**0.4**

ACPD
13, 11827–11862, 2013

Table 2. The low-level flux budget of pollutants (NO, NO_2, NO_x and HNO_3) during extreme events over Cape Town, showing the inward and outward fluxes at the west (F_W), east (F_E), south (F_S) and north (F_N) boundaries of Cape Town and the net flux (F_{Net}) over the city. A positive zonal flux (F_E or F_W) implies a westerly flux (i.e. a flux from west direction) while a negative zonal flux means the opposite. A positive meridional flux (F_N or F_S) denotes a southerly flux (i.e. a flux from south direction) while a negative zonal flux means the opposite. Inward fluxes (from any boundary or direction) into the city are in red, while outward fluxes from the city are in black. A positive F_{Net} indicates divergence (i.e. depletion) of the pollutants over the city while a negative net flux means convergence (i.e. accumulation) of the pollutants over the city.

	NO		NO_2		NO_x	HNO_3		
	Mar	Apr	Mar	Apr	Apr	Mar	Apr	May
F_W	−3.1	−0.4	−0.9	−1.0	−0.7	1.4	−0.5	1.0
F_E	−3.0	−0.7	−0.5	−0.9	−1.4	1.3	0.7	1.1
F_S	0.8	−0.9	0.5	0.1	−0.8	−0.8	1.8	−0.6
F_N	−1.1	−2.0	−0.6	−1.1	−1.6	−0.4	0.8	−1.0
F_{Net}	**−1.8**	**−1.3**	**−0.7**	**−1.1**	**−1.4**	**0.3**	**0.2**	**−0.3**

ACPD
13, 11827–11862, 2013

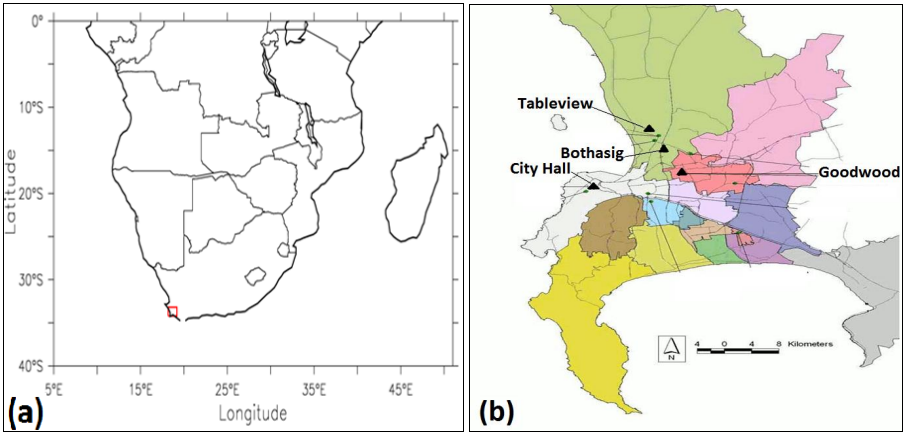

Fig. 1. Study domain: **(a)** map of southern Africa showing Cape Town area (red box) at the south western tip of South Africa; **(b)** the City of Cape Town air quality network showing the location of four observation stations (Bothasig, City Hall, Goodwood and Tableview) used in the study (source: http://web1.capetown.gov.za/web1/cityairpol/, with some modifications).

ACPD
13, 11827–11862, 2013

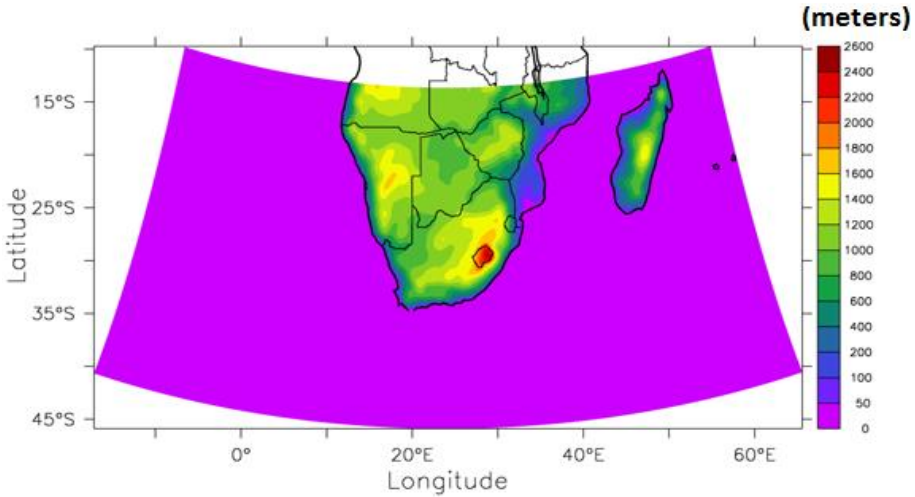

Fig. 2. RegCM simulation domain indicating the topography of southern Africa as seen by the model.

ACPD
13, 11827–11862, 2013

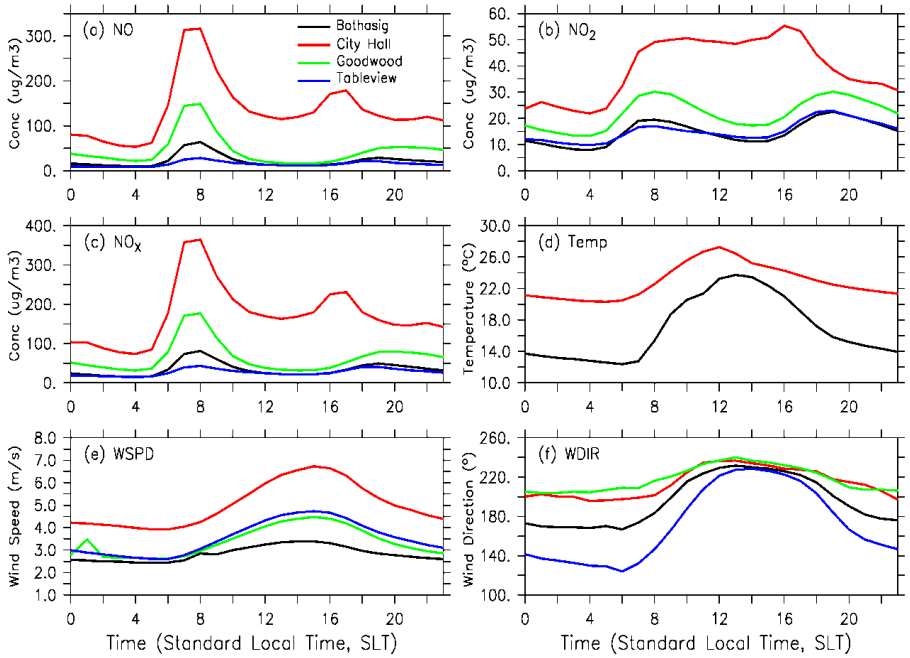

Fig. 3. Diurnal variation of observed **(a)** NO, **(b)** NO_2, **(c)** NO_x, **(d)** temperature, **(e)** wind speed, and **(d)** wind direction at four monitoring stations in Cape Town.

ACPD
13, 11827–11862, 2013

Transport of atmospheric NO_x and HNO_3 over Cape Town

B. J. Abiodun et al.

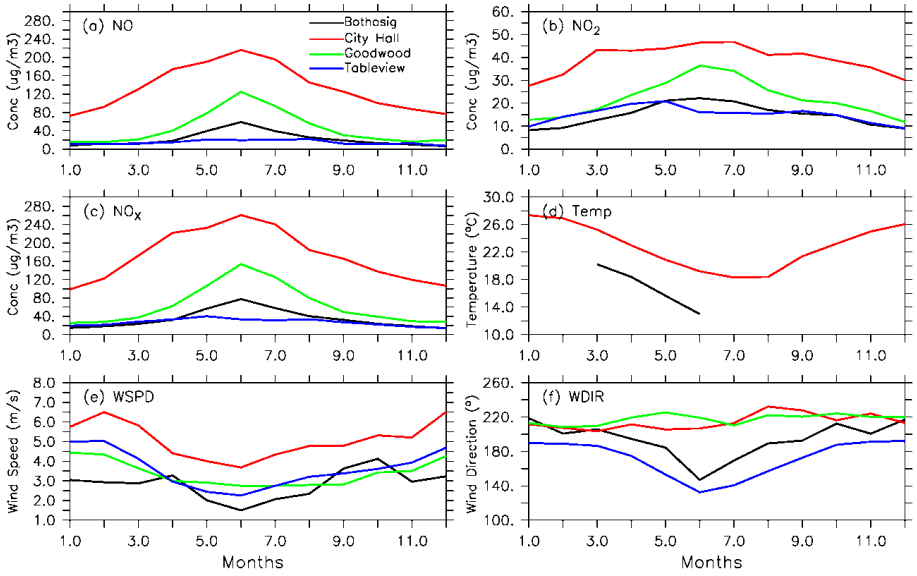

Fig. 4. The seasonal variation of observed **(a)** NO, **(b)** NO_2, **(c)** NO_x, **(d)** temperature, **(e)** wind speed, and **(d)** wind direction at four monitoring stations in Cape Town.

ACPD
13, 11827–11862, 2013

Transport of atmospheric NO_x and HNO_3 over Cape Town

B. J. Abiodun et al.

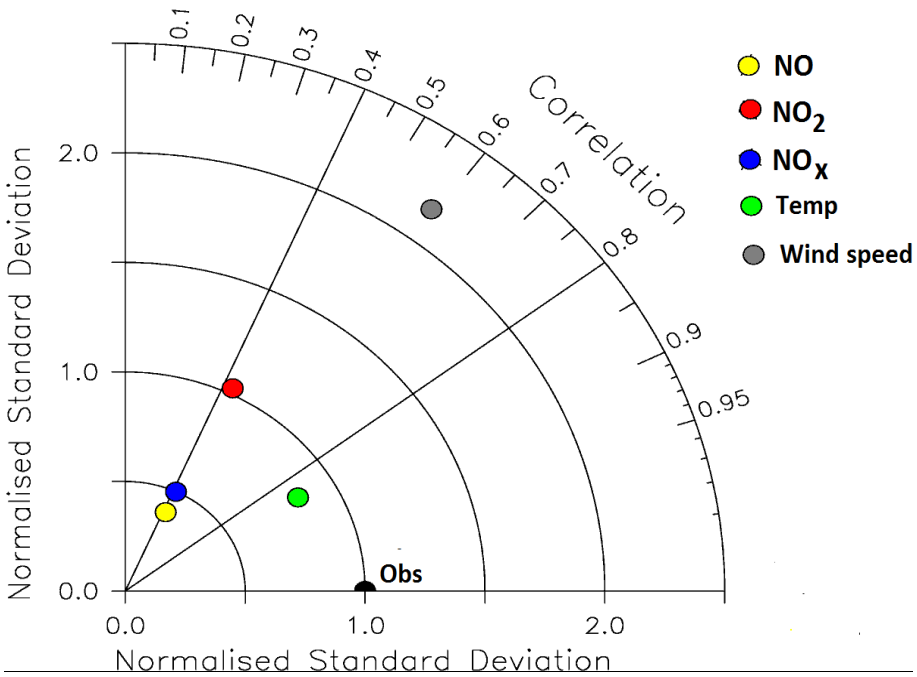

Fig. 5. Comparison of the simulated (RegCM4) daily mean concentration of NO, NO_2 and NO_x temperature (Temp), and wind speed with the observed (Obs).

ACPD
13, 11827–11862, 2013

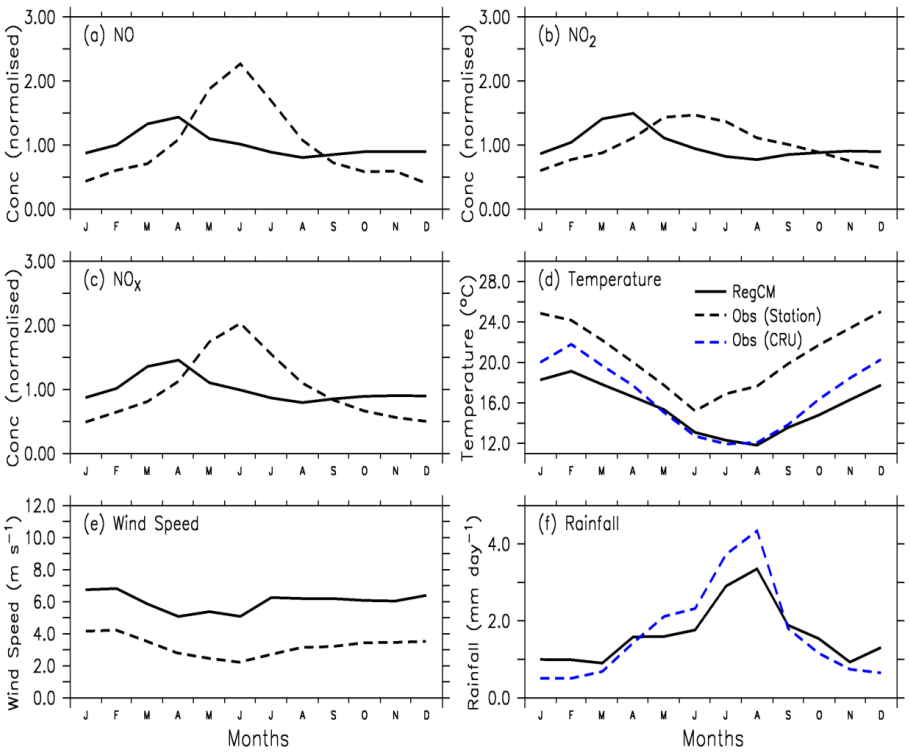

Fig. 6. Seasonal variation of observed and simulated **(a)** NO, **(b)** NO_2, **(c)** NO_x, **(d)** temperature (°C), **(e)** wind speed ($m\,s^{-1}$), and **(f)** rainfall ($mm\,day^{-1}$). The NO, NO_2 and NO_x are normalised with their annual mean values.

ACPD
13, 11827–11862, 2013

Transport of atmospheric NO_x and HNO_3 over Cape Town

B. J. Abiodun et al.

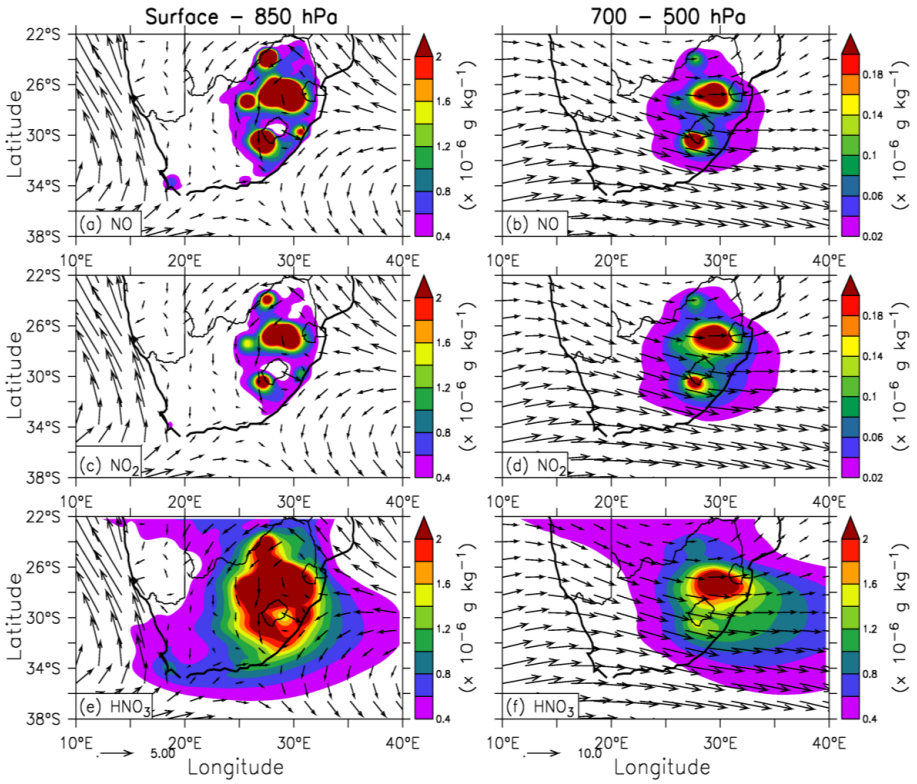

Fig. 7. RegCM4 simulated annual mean (2001–2004) concentration for NO ($\times 10^{-6}$ g kg^{-1}; top panels), NO_2 ($\times 10^{-6}$ g kg^{-1}; middle panels) and HNO_3 ($\times 10^{-6}$ g kg^{-1}; bottom panels) at low-level (surface–850 hPa; left panels) and middle-level (700–500 hPa; right panels) over South Africa. The corresponding wind speeds are shown with arrows; the arrows at bottom of the bottom panels (**e** and **f**) show the wind scale of 5 m s^{-1} and 10 m s^{-1}, respectively.

ACPD
13, 11827–11862, 2013

Transport of atmospheric NO_x and HNO_3 over Cape Town

B. J. Abiodun et al.

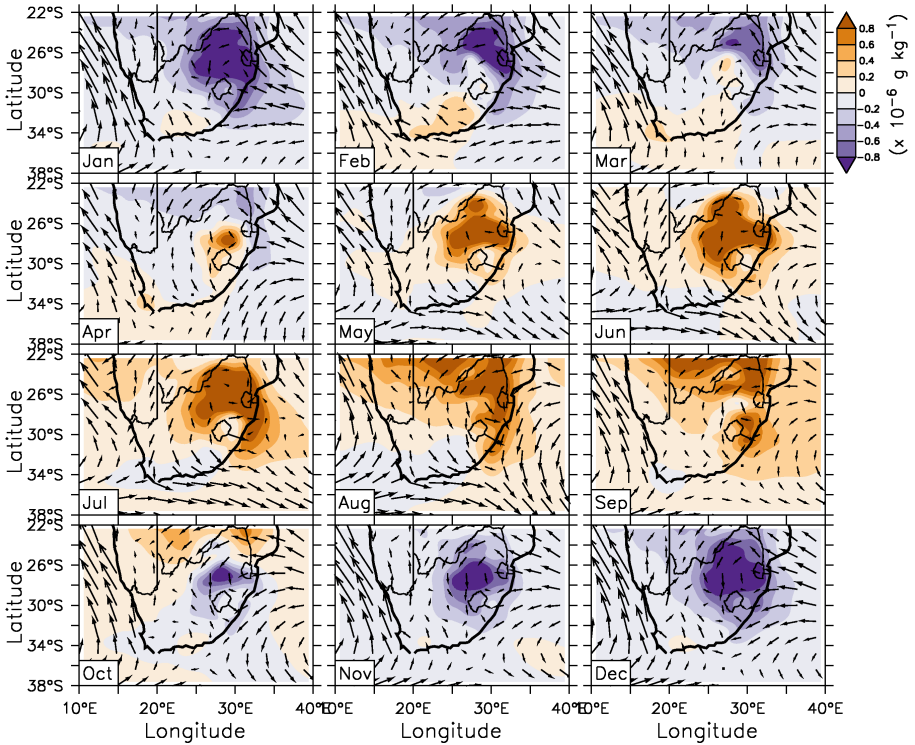

Fig. 8. Monthly anomalies of the simulated HNO_3 concentration ($\times 10^{-6}\,g\,kg^{-1}$) over South Africa.

ACPD
13, 11827–11862, 2013

Transport of atmospheric NO_x and HNO_3 over Cape Town

B. J. Abiodun et al.

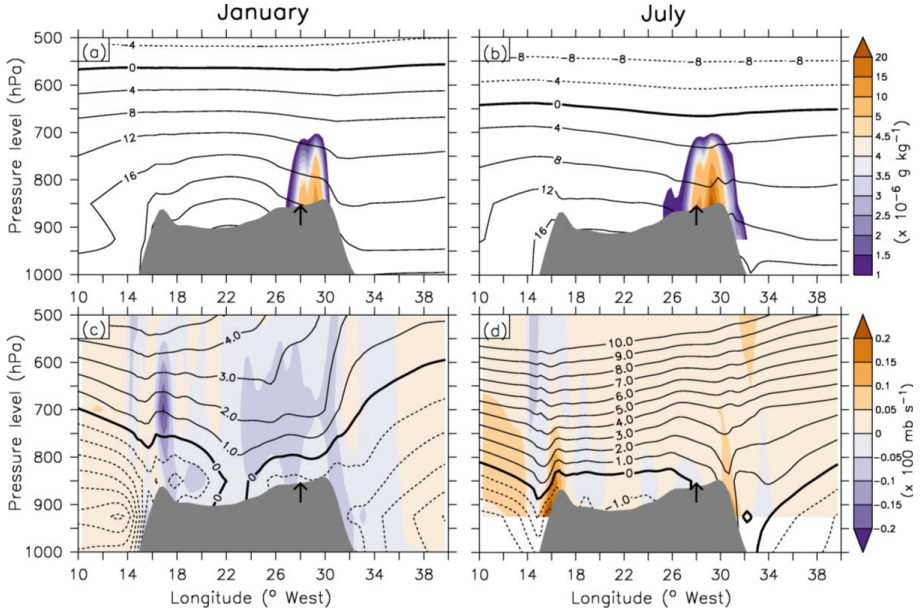

Fig. 9. Vertical cross section of HNO_3 concentration ($\times 10^{-6}$ g kg^{-1}; shaded in upper panels) and temperature (°C; contours in upper panels), vertical wind component ($\times$ 100 mb s^{-1}; shaded in lower panels), and zonal wind component (m s^{-1}; contours in lower panels) at latitude 26° S in January and July. Topography is shown in grey colour and the location of the Highveld indicated with arrow (↑).

ACPD
13, 11827–11862, 2013

Transport of atmospheric NO_x and HNO_3 over Cape Town

B. J. Abiodun et al.

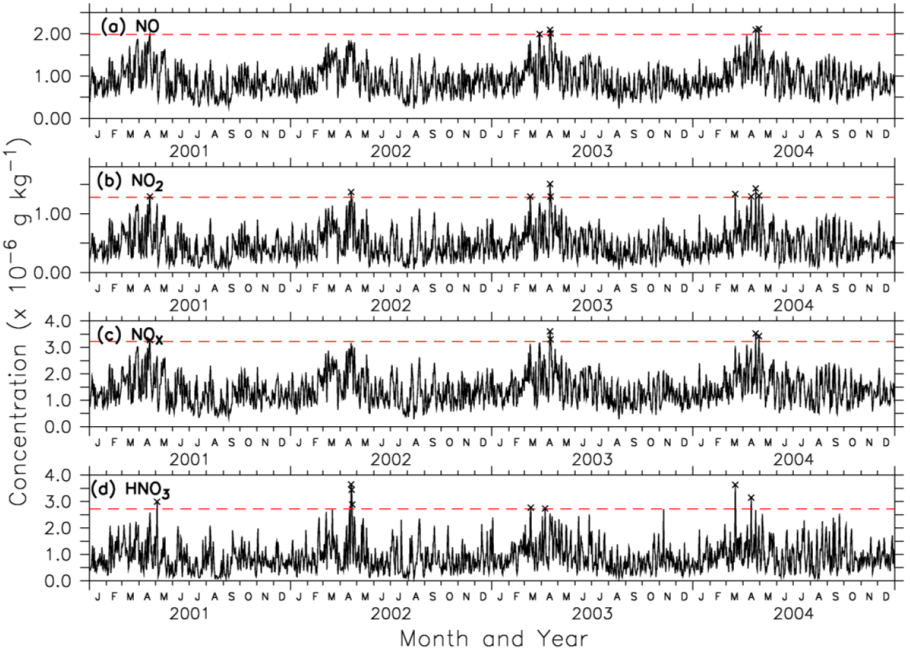

Fig. 10. The time series of the simulated pollutants concentration over Cape Town in 2001–2004. The extreme values (99 percentiles) are indicated with red dashed.

ACPD
13, 11827–11862, 2013

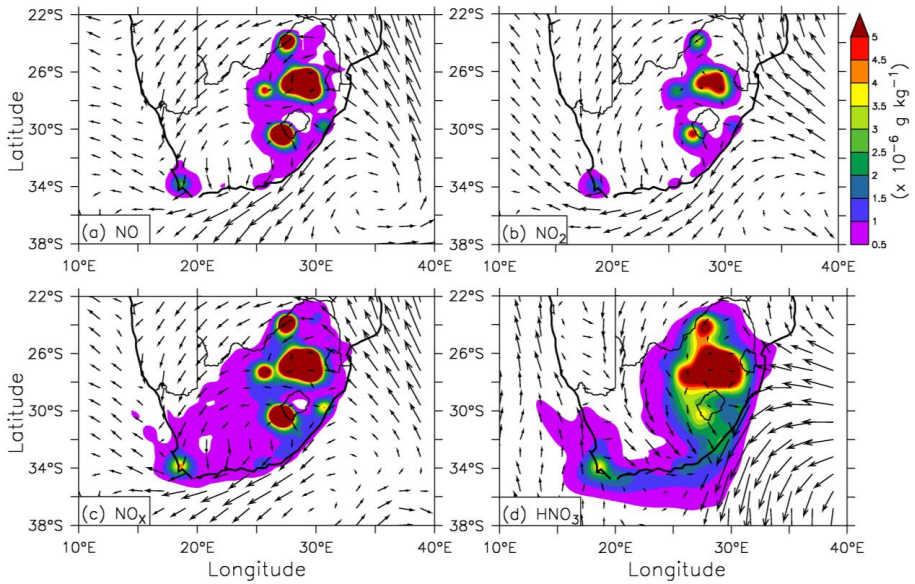

Fig. 11. The composite of low-level (surface–850 hPa) wind flow (arrow) during the extreme pollution events in Cape Town. The corresponding pollutant concentration (NO, NO2, NO_x and HNO3; $\times 10^{-6}\,g\,kg^{-1}$) are shaded.

ACPD
13, 11827–11862, 2013

Transport of atmospheric NO_x and HNO_3 over Cape Town

B. J. Abiodun et al.

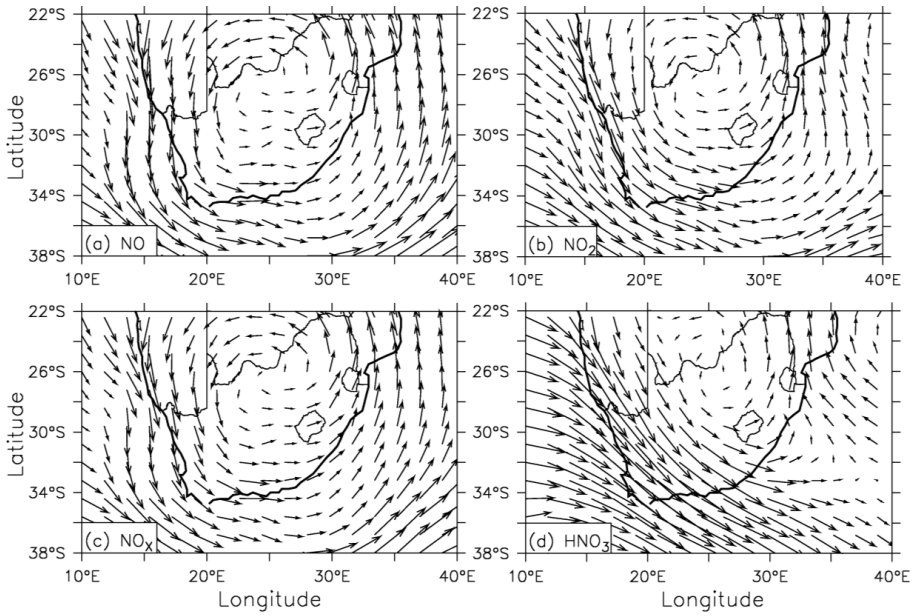

Fig. 12. The composite of 700 hPa wind flow during extreme events of pollutants (NO, NO_2, NO_x and HNO_3) concentration at surface in Cape Town.

ACPD
13, 11827–11862, 2013